

Reaction ensemble Monte Carlo technique and hypernetted chain approximation study of dense hydrogen

V. Bezkrovniy,¹ M. Schlanges,¹ D. Kremp,² and W. D. Kraeft¹

¹*Institut für Physik, Ernst-Moritz-Arndt-Universität Greifswald, Domstrasse 10a, D-17487 Greifswald, Germany*

²*Fachbereich Physik, Universität Rostock, Universitätsplatz 3, D-18051 Rostock, Germany*

(Received 3 June 2003; published 16 June 2004)

In spite of the simple structure of hydrogen, up to now there is no unified theoretical and experimental description of hydrogen at high pressures. Recent results of Z-pinch experiments show a large deviation from those obtained by laser driven ones. Theoretical investigations including *ab initio* computer simulations show considerable differences at such extreme conditions from each other and from experimental values. We apply the reaction ensemble Monte Carlo technique on one hand and a combination of the hypernetted chain approximation with the mass action law on the other to study the behavior of dense hydrogen at such conditions. The agreement between both methods for the equation of state and for the Hugoniot curve is excellent. Comparison to other methods and experimental results is also performed.

DOI: 10.1103/PhysRevE.69.061204

PACS number(s): 51.30.+i, 05.70.Ce, 64.30.+t, 02.70.Uu

I. INTRODUCTION

The equation of state (EOS) of dense hydrogen and its isotopes covers regions from the fully ionized plasma, consisting of electrons and protons, to atomic and molecular hydrogen being in fluid and solid state. At high temperatures and pressures, the system consists of free electrons and protons. Decreasing temperature leads to the formation of bound states such as atoms H, molecules H₂, molecular ions H₂⁺, and other species. Such a partially ionized plasma is the object of many theoretical investigations by using analytical methods [1–11] and computer simulation techniques [12–21]. Especially such investigations become more important in connection with shockwave experiments [22–27] which give the most reliable information on the EOS for hydrogen at extreme conditions.

During shockwave experiments the system goes through different thermodynamic states accompanied by molecular dissociation, ionization, electron excitation, and other processes. The difficulty of the consistent theoretical description of all these processes is well known. That is why some theories are restricted only to the regions of completely ionized hydrogen [4,9] or to the neutral system, consisting of a mixture of molecular and atomic hydrogen [11]. As a result these theories agree with the experimental data only in definite regions of the equation of state and therefore of the Hugoniot curve. It seems that among theoretical descriptions only the path integral Monte Carlo (PIMC) method [17] includes consistently all important processes. The results for the Hugoniot curve obtained within the PIMC method are in a good agreement with the Z-pinch experimental results [27] in a wide range of temperatures and densities. But one should mention that at low temperatures, where molecular states dominate a system, the PIMC method converges very slowly to the desired results [15]. The comparison of the PIMC method and the density functional molecular dynamics (DFT-MD) can be found in Ref. [17]. The restrictions of the DFT-MD are also critically discussed in Ref. [28].

Another method which describes the complete region of

the experimental results is the linear mixing model (LM). In contrast to the PIMC method, which is a *first principle* method, the LM was developed to describe shock wave experiments by using parameters fitted to the experimental data, see Ref. [10] and references therein. LM interpolates the EOS between molecular and metallic states of hydrogen.

In view of different experimental results, the compressibility (sixfold) achieved by laser driven experiments [22,23] is not met by Z-pinch experiments [27]; it is interesting to use other theoretical approaches and models in order to investigate how they behave in comparison to the experimental results. Furthermore, we restrict our considerations to a neutral particle system, consisting of molecular and atomic hydrogen. We study the EOS and the Hugoniot curve of hydrogen and deuterium by using reaction ensemble Monte Carlo (REMC) method [29,30]. This is the classical Monte Carlo method which efficiently samples the phase space relevant to chemical reactions, and converges rapidly to the equilibrium densities of reagents and products. The quantum effects can be incorporated in this method by using effective interaction potentials and partition functions of species taking part in chemical reactions. The advantage of this method as compared to widely used approximative methods for the determination of the EOS of hydrogen, such as the Weeks-Chandler-Andersen theory [6] and the fluid variational theory (FVT) [2,11], can be summarized in some points: (i) REMC method calculates the thermodynamic and structural properties more accurately than approximative theories do; (ii) it does not need any reference system; (iii) the application of the REMC method for a system where many chemical reactions occur can be handled by this method in a more effective way than by the usual free energy minimization, or, equivalently, by simultaneous solution of the corresponding mass action laws [31]; and (iv) as recently shown by Brennan and Rice [32], this method can be effectively applied for determining the composition and thermodynamic properties of the shock-compressed materials.

Additionally we have performed calculations by using a combination of hypernetted chain approximations (HNC) and mass action laws (MAL) which we further refer to as

HNC+MAL. The application of HNC for Coulomb systems, as is well known, gives very good results for its equation of state in comparison to Monte Carlo (MC) [33] calculations. Levesque *et al.* [34] studied the application of the integral equation theory, particularly HNC, to the binary nonreacting mixture being under extreme density and pressure. The particles in this mixture interact through the Morse potential. The results for the pressure and other thermodynamic values within the HNC scheme, as found by Levesque *et al.* [34], are very close to those of MC simulations in a wide range of temperatures and densities. It seems to be interesting to investigate whether this performance extends to reacting mixtures of particles interacting through a modified Buckingham EXP6 potential [35].

II. THE MODEL

We consider a reacting mixture consisting of hydrogen molecules and atoms



The hydrogen atoms are chosen to be the basic elements which remain stable under any condition. The interaction between particles is taken into account by the analytical form of the modified Buckingham EXP6 potential [35] as given by Eq. (2)

$$U_{ab}(r) = \frac{\epsilon_{ab}}{\alpha_{ab} - 6} \left\{ \exp \left[\alpha_{ab} \left(1 - \frac{r}{r_{ab}^*} \right) \right] - \alpha_{ab} \left(\frac{r_{ab}^*}{r} \right)^6 \right\} \quad (2)$$

with the parameters $\alpha_{\text{H}_2\text{H}_2} = 11.1$, $\epsilon_{\text{H}_2\text{H}_2}/k_B = 36.4$ K and $r_{\text{H}_2\text{H}_2}^* = 3.43$ Å given by Ross *et al.* [2]. The interaction parameters for hydrogen atoms, $\alpha_{\text{HH}} = 13.0$, $\epsilon_{\text{HH}}/k_B = 20.0$ K, and $r_{\text{HH}}^* = 1.40$ Å, were proposed by Ree [36]. For the interaction between different components, H-H₂, the Lorentz-Berthelot mixing rules was used with $\alpha_{\text{HH}_2} = 12.012$, $\epsilon_{\text{HH}_2}/k_B = 26.98$ K and $r_{\text{HH}_2}^* = 2.415$ Å. For distances $r \rightarrow 0$, where the EXP6 potential shows nonphysical behavior, we used the extrapolation procedure as proposed by Juranek and Redmer [11]. The coefficients for this extrapolation formula can be found in the original papers just mentioned.

The chemical equilibrium between molecules and atoms in Eq. (1) is described by the thermodynamic relation

$$\frac{n_{\text{H}_2}^*}{n_{\text{H}}^{2*}} = K(T) \exp(\beta \Delta \mu), \quad (3)$$

where $n_{\text{H}_2}^*$ and n_{H}^* are the equilibrium densities of molecules and atoms, respectively; $\beta = 1/(k_B T)$. The deviation from ideality is given by the difference $\Delta \mu = 2\mu_{\text{H}}^{\text{int}} - \mu_{\text{H}_2}^{\text{int}}$ of the interaction parts of chemical potentials of the reacting components.

The dissociation constant $K(T)$ in Eq. (3) is introduced as the relation of molecular and atomic partition functions [37], and for a molecule being in ground state it can be written in a general form as

$$K(T) = \frac{\Lambda_A^6}{(2s+1)^2 \sigma \Lambda_M^3} \sum_{n,l} (2l+1) \exp(-\beta E_{nl}). \quad (4)$$

The symbols $A = \text{H}, \text{D}$ and $M = \text{H}_2, \text{D}_2$ correspond to the reacting species, Λ_a , with $a = \text{A}, \text{M}$ the de Broglie wavelength of these species, σ the symmetry number of a molecule, which for hydrogen and deuterium molecules is equal to $\sigma = 2$, and $s = 1/2$ the spin of the electron. The energy levels of the molecule E_{nl} include vibrational and rotational states.

The correct description of the molecular dissociation process requires the knowledge of the accurate vibrational and rotational degrees of freedom of a molecule. In many cases these contributions are treated in the harmonic oscillator approximation as done, for example, in Refs. [2,5,11]. The approximation of the interaction potential by a parabola in the harmonic oscillator approximation leads to the neglect of contributions important, particularly, for large displacements from equilibrium of atoms in a molecule. At the same time the harmonic oscillator possesses an infinite number of energy levels, while the molecule dissociates at a finite energy and also possesses a finite number of vibrational levels only. The improvement as compared to the harmonic oscillator is usually done by taking into account more than one term in a Taylor series of the expansion of the potential energy near equilibrium distance. These terms describe anharmonicity effects and also coupling between vibrational and rotational motion. But because of the infinite number of expansion terms in a Taylor series it is not quite clear how many terms should be taken into account [38].

In order more strictly to take into account anharmonicity and coupling between rotational and vibrational motion we solved the Schrödinger equation with the potential calculated by Kolos and Wolniewicz [39] and fitted to the analytical form of the Murrell-Sorbie potential by Liu *et al.* [40],

$$U_{\text{HH}}(r) = -D_e(1 + a_1\rho + a_2\rho^2 + a_3\rho^3) \exp(-a_1\rho), \quad (5)$$

where $\rho = r - r_{\text{min}}$, $D_e = 4.747$ eV, $r_{\text{min}} = 0.7414$ Å, $a_1 = 3.961$ Å⁻¹, $a_2 = 4.064$ Å⁻², $a_3 = 3.574$ Å⁻³. The results for rotational and vibrational energy levels E_{nl} of hydrogen and deuterium molecules are in excellent agreement with the experimental results of Herzberg and Howe [41] and Stoich-eff [42]. We also found a good agreement with results of Patch [43], Wolniewicz [44], and Waech and Bernstein [45] who have done similar calculations.

In Fig. 1, results for the vibrational energy levels of hydrogen and deuterium molecules for the angular quantum number $l = 0$ are shown. For comparison, also those levels in the harmonic oscillator approximation are shown corresponding to molecular parameters θ_v introduced in Table I. As we can expect, the harmonic oscillator approximation is valid only for the ground vibronic state and at most for the first excited states of the molecule. Because of the lighter

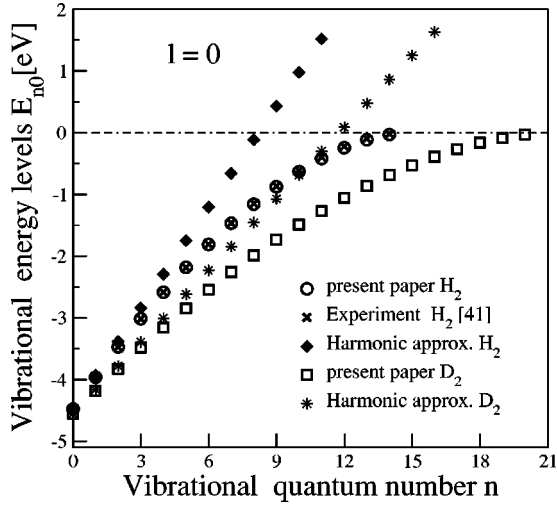


FIG. 1. Solutions of the Schrödinger equation for vibrational energy levels of molecular hydrogen and deuterium for the orbital quantum number $l=0$. The results are compared to the energy levels in harmonic oscillator approximation.

mass, the vibrational energy levels of the hydrogen molecule converge quicker to the continuum line $E_{n0}=0$ than those of the deuterium one. There is an infinite number of energy levels calculated in the framework of the harmonic oscillator approximation going beyond the continuum line. This is due to the application of a confined potential.

Because of the well known problem of the definition of bound states, starting from the physical picture, we want to mention that the definition of the mass action law by Eq. (4) is not the only possibility. It is more useful to introduce the dissociation constant according to

$$K(T) = \frac{\Lambda_A^3}{2\sqrt{2}} \sum_{n,l} (2l+1) [\exp(-\beta E_{nl}) - 1]. \quad (6)$$

This formula is justified by the application of the Levinson theorem to the singlet part of the quantum virial coefficient [46]. The energy levels E_{nl} in Eq. (6) are those calculated from the Schrödinger equation with the interaction potential (5) according to Ref. [39].

Next we compare results for the degree of dissociation $\alpha = n_H^*/(n_H^* + 2n_{H_2}^*)$, calculated from Eq. (3) using Eq. (6) and the expression for dissociation constant $K_h(T)$ in harmonic oscillator approximation

$$K_h(T) = \frac{\Lambda_A^3}{2\sqrt{2}} \frac{T}{\theta_r} \frac{\exp(\beta D_0)}{1 - \exp(-\beta \theta_v)}, \quad (7)$$

TABLE I. Constants for hydrogen and deuterium molecules [47].

	D_0 (K)	θ_v (K)	θ_r (K)
H ₂	51930.0	6332.05	87.55
D ₂	52835.3	4486.68	43.78

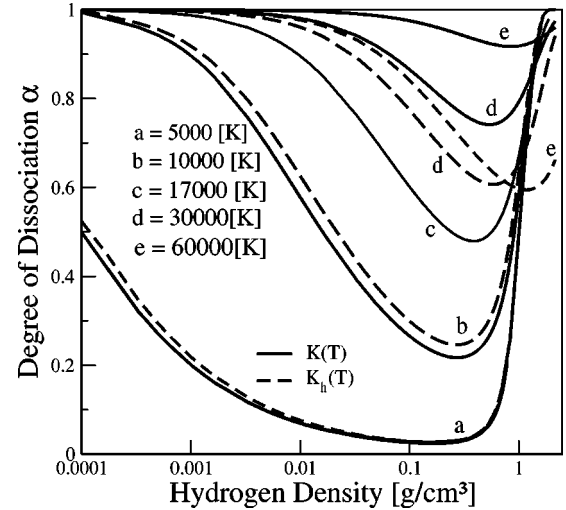


FIG. 2. Degree of dissociation α for molecular hydrogen in anharmonic approximation (6) and harmonic approximation (7). Calculations were done in the HNC+MAL scheme. At $T = 17\,000$ K, harmonic and anharmonic results coincide.

where the values for the dissociation energy D_0 , the rotational θ_r and the vibrational θ_v constants are given in Table I. The calculations for $\Delta\mu$ were done in the framework of the HNC+MAL method.

As we can see from Fig. 2 for the temperatures $T=5000$ and $10\,000$ K, where the main contribution to the dissociation constant comes from the ground vibrational state, the agreement of α calculated by using Eqs. (6) and (7) is rather good. With increasing temperature the discrepancy of the results becomes more pronounced, then the difference between harmonic and anharmonic results changes the sign after passing zero for about $T=17\,000$ K. At $T=60\,000$ K, using Eq. (6), we obtain almost completely dissociated molecular hydrogen. The result with $K_h(T)$ shows strong formation of molecules at this temperature (note that the binding energy for the isolated hydrogen molecule is $D_0 = 51\,930$ K). The reason is that, for large temperatures, $K_h(T)$ increases asymptotically as $K_h(T) \approx \sqrt{T}$ where, at the same conditions, we have $K(T) \rightarrow 0$.

The difference of the masses of hydrogen and deuterium molecules, $m_{D_2} = 2m_{H_2}$, has an influence on the number of rotational and vibrational levels E_{nl} from solutions of the Schrödinger equation but produces a very small effect on the dissociation constants of both elements. It seems that all effects in Eq. (6) compensate each other and the final result is not sensitive to such difference in the masses. As we can see from Table II, only at low temperatures there is some discrepancy in the dissociation constants for hydrogen and deuterium, but, with increasing temperature, this discrepancy practically vanishes.

III. NUMERICAL METHODS AND DETAILS OF SIMULATIONS

A. Reaction ensemble Monte Carlo

The simulation in the framework of the REMC method was done at constant volume V and temperature T for both

TABLE II. Dissociation constants, Eq. (6), for hydrogen and deuterium.

T (K)	K_{D_2} (\AA^3)	K_{H_2} (\AA^3)
2000	12×10^{10}	10×10^{10}
5000	17002	16556
8000	383.85	380.21
10000	108.79	108.14
30000	1.7635	1.7610
60000	0.2447	0.2445
100000	0.0609	0.0609

hydrogen and deuterium. At these conditions the method generates two types of state transitions: particle displacements P^{dis} and reaction steps P^r .

The particle displacements are implemented in the usual way with the transition probability

$$P^{dis} = \min[1, \exp(-\beta\Delta U)], \quad (8)$$

where ΔU is the change in the configurational energy of particles interacting through the EXP6 potential Eq. (2).

The reaction step for molecular hydrogen dissociation Eq. (1) is given by

$$P^r = \min\left[1, \exp(-\beta\Delta U) \frac{N_{H_2} V}{(N_H + 2)(N_H + 1)K(T)}\right], \quad (9)$$

where $K(T)$ is the dissociation constant Eq. (6), N_H and N_{H_2} are the numbers of hydrogen atoms and molecules, respectively.

The reverse reaction in Eq. (1) is accepted with the probability

$$P^r = \min\left[1, \exp(-\beta\Delta U) \frac{N_H H(N_H - 1)K(T)}{(N_{H_2} + 1)V}\right]. \quad (10)$$

It is necessary to mention that REMC includes automatically the condition of the chemical equilibrium, Eq. (3), in its reaction transition probabilities, Eqs. (9)–(10).

The thermodynamic data such as pressure p and the configurational part of the internal energy U^{int} were calculated as averages over configurational states [48]

$$p = \sum_a \frac{\langle N_a \rangle}{V} k_B T - \frac{1}{3V} \left\langle \sum_{a,b} \sum_{i < j} \frac{U_{ab}(r_{ij})}{dr_{ij}} r_{ij} \right\rangle, \quad (11)$$

$$U^{int} = \left\langle \sum_{a,b} \sum_{i < j} U_{ab}(r_{ij}) \right\rangle \langle N \rangle k_B T. \quad (12)$$

The simulations were performed in a cubic simulation box with the minimum image convention, with periodic boundary conditions, and with a cutoff radius equal to half the box length. The initial configuration was taken to be the face-centered-cubic (fcc) lattice for every input total hydrogen density $n_t = n_H^* + 2n_{H_2}^*$. For densities $n_t \leq 0.1$ g/cm³, the initial number of hydrogen atoms and molecules was taken to

be equal to $N_H = N_{H_2} = 54$. For densities $n_t > 0.1$ g/cm³ the initial number of molecules and atoms was $N_H = N_{H_2} = 250$.

In the course of the simulations, the numbers of particles (atoms and molecules) for any given n_t changed due to reactions, the box volume had to be calculated for every input total hydrogen density n_t . The maximum number of particles for complete dissociated hydrogen was 162 for $n_t \leq 0.1$ g/cm³ and 750 for $n_t > 0.1$ g/cm³. The acceptance rate for particle moves was set to be 30%. The EXP6 potential long range corrections for the configurational energy and pressure were included, assuming that the radial distribution function is unity beyond the cutoff distance.

For the calculation of averages, Eqs. (11) and (12), and for the composition, the system was equilibrated by 10⁷ steps, and the same number of steps was used for the production cycles. The final results were obtained as the mean over 20 blocks.

B. Hypernetted chain approximation and mass action law

Let us consider the HNC with the MAL for reacting systems. We obtained values for the direct correlation function $c_{ab}(r)$ and for the total correlation function $h_{ab}(r)$ from the solution of the Ornstein-Zernicke equation for mixtures

$$h_{ab}(r) = c_{ab}(r) + \sum_k n_k \int c_{ak}(|\mathbf{r} - \mathbf{r}'|) h_{kb}(\mathbf{r}') d\mathbf{r}', \quad (13)$$

with the HNC closure relation for the direct correlation function

$$c_{ab}(r) = -\beta U_{ab}(r) + \ln[h_{ab}(r) + 1] + h_{ab}(r), \quad (14)$$

and with the interaction potential $U_{ab}(r)$ given by Eq. (2). With these results the interaction parts of the chemical potentials in the HNC approximation [49] were calculated

$$\beta \mu_a^{int} = \sum_b n_b^* \int \left(\frac{1}{2} h_{ab}(\mathbf{r}) [h_{ab}(\mathbf{r}) - c_{ab}(\mathbf{r})] - c_{ab}(\mathbf{r}) \right) d\mathbf{r}. \quad (15)$$

The values for the interaction parts of the chemical potentials of molecular and atomic hydrogen were substituted into the expression for the MAL, which we rewrite in a slightly different version of Eq. (3),

$$\frac{1 - \alpha}{\alpha^2} = 2n_t K(T) \exp(\beta \Delta \mu). \quad (16)$$

The degree of dissociation was calculated by an iterative procedure which was terminated after a given value $|(\alpha_{j+1} - \alpha_j)/\alpha_{j+1}| < 10^{-4}$ was reached.

For the calculation of the total and direct correlation functions, Eqs. (13) and (14), the Ornstein-Zernicke equation was solved by using the Gillan algorithm [50] which we adopted to many component systems. The direct correlation functions

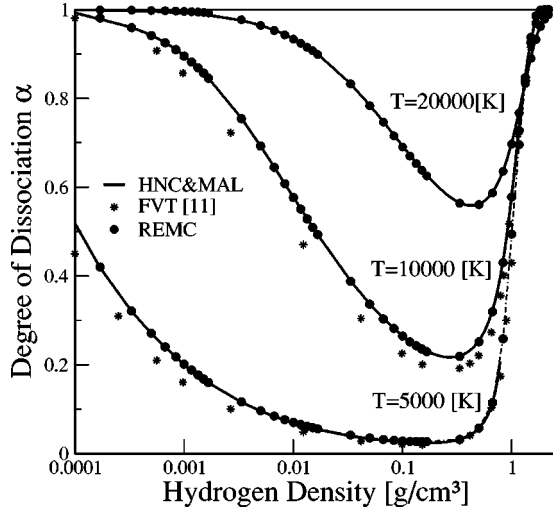


FIG. 3. Degree of dissociation α for molecular hydrogen calculated by HNC+MAL and REMC methods. Comparison to FVT [11] is also given. At $T=5000$ K, the HNC+MAL result is terminated at the density 0.78 g/cm^3 . This indicates the region where we did not find solutions to the OZ equation.

$c_{ab}(r)$ and the total correlation functions $h_{ab}(r)$ were calculated on an equidistant grid space with $N=2048$ points and a step $\Delta r=0.025 \text{ \AA}$.

The pressure and the configurational part of the internal energy in the HNC+MAL approximations are calculated by using the radial distribution function $g_{ab}(r)=h_{ab}(r)+1$,

$$p = \sum_a n_a^* k_B T - \frac{2\pi}{3} \sum_{a,b} n_a^* n_b^* \int_0^\infty \frac{dU_{ab}(r)}{dr} g_{ab}(r) r^3 dr, \quad (17)$$

$$U^{int}/Nk_B T = 2\pi \sum_a \sum_b x_a x_b \int_0^\infty U_{ab}(r) g_{ab}(r) r^2 dr, \quad (18)$$

where $x_c = n_c / \sum_b n_b$ is the fraction of the component c .

IV. RESULTS

In the scheme presented in this paper we consider only molecular dissociation, neglecting ionization. This restricts the application of the theory to temperatures and densities where the ionization is small and its effect on the thermodynamic properties can be neglected.

The degree of dissociation as a function of the total hydrogen density n_t for some temperatures is presented in Fig. 3. Both methods, REMC and HNC+MAL, show a similar behavior for all temperatures and densities. For low temperatures we have found that there are regions in the n - T plane, like in the case $T=5000$ K, where no solutions of the Ornstein-Zernicke equation exist. This can indicate the appearance of instabilities in the system. Such instabilities at low temperatures for systems with EXP6 interactions were reported by Ree [36], and by Juranek and Redmer [11]. Results for the degree of dissociation calculated within the FVT [11] are close to ours at $T=5000$ K, but for the temperature

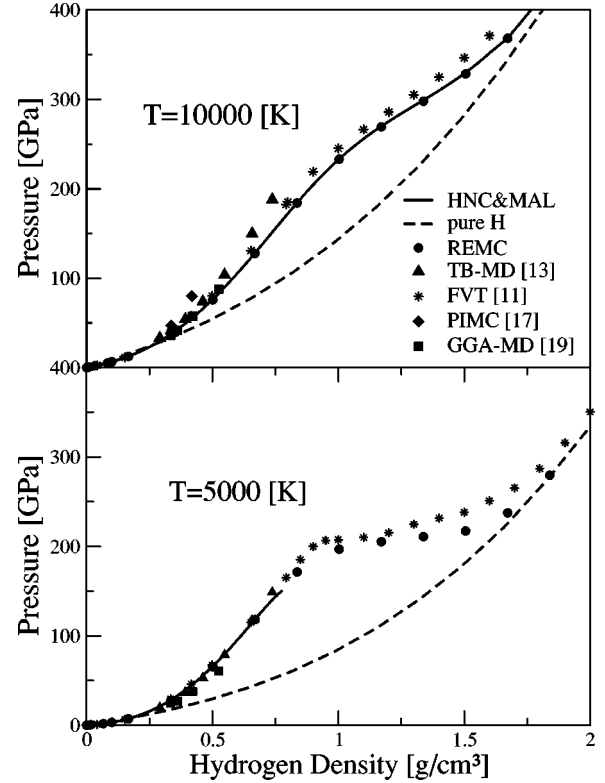


FIG. 4. Hydrogen pressure vs density. At $T=5000$ K the curve for HNC+MAL method terminates at the same density as explained in Fig. 3. Comparison to other theories is shown.

$T=10000$ K, they lie below ours. It means that the molecular partition function used in the FVT produces more molecules than our procedure does at given temperature and density.

It should be noted that, with increasing temperature, the minimum of the degree of dissociation is shifted to higher densities. At the same time α increases less rapidly at higher temperatures than at lower ones (see also Fig. 2). This is a consequence of the decreasing nonideality effects at such temperatures because of the competition between particle interactions and their thermal motion.

Comparing the results for the pressure calculated by REMC and HNC+MAL methods we found that they almost coincide for all temperatures and densities, except for regions where HNC does not give solutions of the Ornstein-Zernicke equation. Some results for $T=5000$ and 10000 K are introduced in Fig. 4. At the temperature $T=5000$ K both REMC and HNC+MAL methods show very good agreement with FVT [11] and tight-binding molecular dynamics (TB-MD) [13]. Pressures calculated within a generalized gradient approximation molecular dynamics (GGA-MD) [19] are lower than those of REMC method and of HNC+MAL method. At $T=10000$ K and densities up to 0.5 g/cm^3 , our results and those of FVT, and of TB-MD, lie close to each other. Better agreement is also achieved in comparison to the results of GGA-MD. Militzer and Ceperley [17,18], who used (PIMC) simulations, reported higher pressures for this temperature than REMC and HNC+MAL methods.

The dissociation from molecular to atomic hydrogen oc-

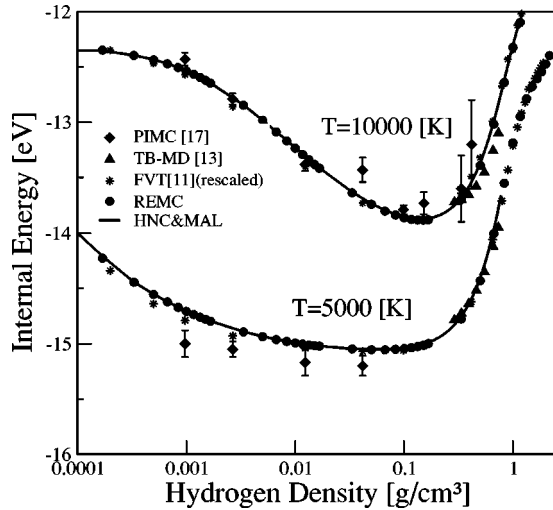


FIG. 5. Dependence of the internal energy on the hydrogen density. Values for the internal energy according to FVT [11] were rescaled to the ground state energy of the hydrogen atom $I = -13.6$ eV. Comparison to other theories is shown.

curs continuously and this in turn leads to changing the pressure of mixtures of two components to the pressure of pure atomic hydrogen as shown in Fig. 4. Because of the restrictions of the model considered in this paper, the atomic hydrogen does not undergo phase transitions to a metallic one with increasing pressure [51,52] and stays as a dense atomic fluid.

In order to compare our results for the internal energy with those of the *ab initio* computer simulations we have normalized the internal energy in REMC and HNC+MAL methods to the ground-state energy of the isolated hydrogen atom $I = -13.6$ eV. The internal energy per atom in eV is given by

$$E = \left(\frac{3}{2} k_B T + x_{H_2} E_{mol} + U^{int} \right) / (2 - x_H) - 13.6, \quad (19)$$

where U^{int} was calculated within REMC or HNC+MAL method. The contribution of the internal degrees of freedom of a molecule to the internal energy is

$$E_{mol} = \frac{\sum_{n,l} (2l+1) E_{nl} \exp(-\beta E_{nl})}{\sum_{n,l} (2l+1) [\exp(-\beta E_{nl}) - 1]}. \quad (20)$$

Like in the case of density and pressure, the results for the internal energy, calculated by REMC and HNC+MAL methods, practically cannot be distinguished on the scale introduced in Fig. 5. For the temperatures $T = 5000$ and 10000 K, REMC and HNC+MAL methods agree very well with PIMC [13] and TB-MD methods [8]. The results of the FVT [11] rescaled to the ground state energy of isolated hydrogen atom are also very close to our data.

We have also used our EOS data to derive the Hugoniot curve for shocked liquid deuterium. The Hugoniot curve is

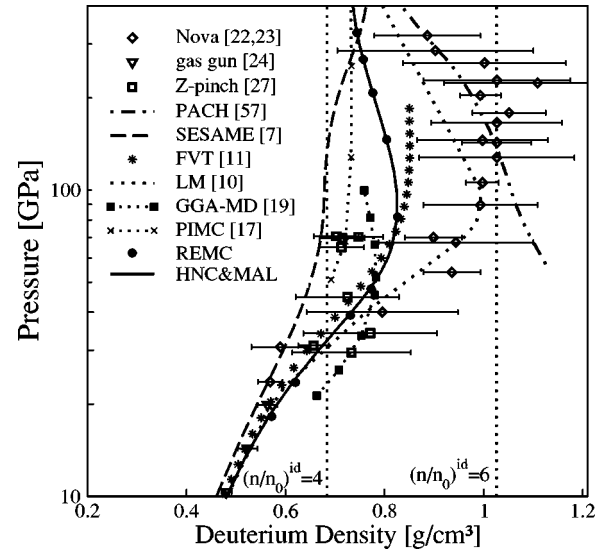


FIG. 6. Comparison of experimental results with Hugoniot curves derived from different EOS models.

the locus of final conditions with the density n , pressure p , and energy E that can be reached with shocks of increasing intensity from a fixed initial state with density n_0 , pressure p_0 , and energy E_0 . The relation between initial and final conditions is given by the Hugoniot equation

$$E = E_0 + \frac{1}{2} (p + p_0) \left(\frac{1}{n_0} - \frac{1}{n} \right). \quad (21)$$

For the calculation of the Hugoniot curve, the initial state was taken to be liquid deuterium with the the initial density $n_0 = 0.171$ g/cm³. This value is typical for experimental conditions [22–27]. We ignore the very small initial pressure p_0 , setting $p_0 = 0$. The initial energy was taken to be $E_0 = -15.875$ eV/atom which is the sum of the ionization energy of the deuterium atom $I = -13.6$ eV/atom and a half of the dissociation energy of the deuterium molecule $D_0/2 = -2.275$ eV/atom.

As we expected, the solutions of the Hugoniot equation (21) for both REMC and HNC+MAL methods differ only about a few percent (maximum 1%). As shown in Fig. 6, the Hugoniot curve calculated within the HNC+MAL method goes practically through all points of the REMC method. In the low pressure region our results are close to the gas gun experiment data given by Nellis *et al.* [24] and to the Z-pinch data by Knudson *et al.* [27]. But with increasing pressure, our data tend to the experimental values found by Da Silva *et al.* [22] and by Collins *et al.* [23] which used laser driven experimental techniques. The maximum compression predicted by our calculation is $n/n_0 = 4.82$ which differs from the laser driven experimental value $n/n_0 = 6$ and at the same time from the Z-pinch results. At the point of maximum compression our theory predicts the temperature $T = 20000$ K which is almost two times higher than the temperature obtained experimentally, using pyrometric measurements of single-shock-compressed liquid deuterium, by Collins *et al.* [58].

It is important to note that for pressures higher than 30 GPa the difference between data obtained by different experimental techniques increases. On one hand, the data of Belov *et al.* [59], who used the high explosive sphere experimental technique, and those of Knudsen *et al.* [27], lie close to each other and to the results of the database SESAME and those of the PIMC method. On the other, high compressibility achieved by laser driven experiments is supported only by the linear mixing model of Ross [10]. Such a situation shows that there is still theoretical work to do in order to understand such behavior.

Comparison of our results to other theoretical methods and *ab initio* computer simulations shows a good agreement with FVT [11] and with the LM [10] in the low pressure regime. Discrepancy to SESAME [7], which is widely used as a standard EOS, increases rapidly with increasing pressure. The values for the Hugoniot curve calculated within the PIMC method [17] lie close to the line $n/n_0=4$ and agree with our data only at high temperatures and pressures. But such agreement is rather the result of the correct asymptotic behavior of our model than the description of real processes in this region. The results by Collins *et al.* [19] within GGA-MD method show a maximum compressibility $n/n_0=4.58$ which is close to our value. However, the general position of the GGA-MD Hugoniot curve in the P - n plane in Fig. 6 differs substantially from our results.

As we already mentioned, at high temperatures, the Hugoniot curve calculated within our model shows the correct limiting compressibility $n/n_0=4$ [53–55]. After the dissociation of molecular deuterium was completed, further increase of the temperature leads only to an increasing kinetic energy of atomic deuterium and diminishing of the influence of interaction between particles. At temperatures high enough, atoms behave like ideal particles with the result that $n/n_0=4$. This result is a consequence of the adequate description of the molecular partition function for deuterium. It becomes more pronounced if we compare the Hugoniot curves calculated by using the harmonic oscillator approximation for the dissociation constant Eq. (7). For this calculation the expression for the internal energy E in Eq. (21) was also used in the harmonic oscillator approximation [56]. The results for the limiting behavior of the Hugoniot curve at high temperatures are introduced in Fig. 7. The nonphysical formation of deuterium molecules at high temperatures $T > T_D$ causes an increasing compressibility to the limiting value $n/n_0=8$. This is the maximum compressibility of the ideal molecular gas with harmonic oscillations which is out of the range of all experimental values.

V. SUMMARY

We have applied REMC and HNC+MAL methods for describing the equation of state of dense hydrogen and the Hugoniot curve for deuterium. Although the HNC equation

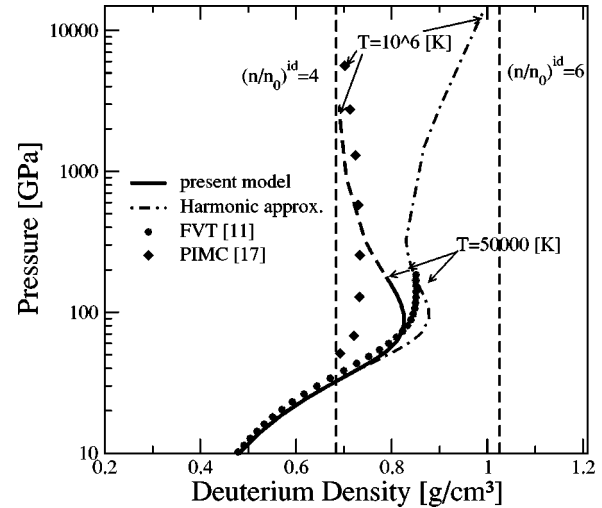


FIG. 7. Influence of the anharmonic approximation, Eq. (6), and harmonic approximation, Eq. (7) on the limiting behavior of the Hugoniot curve at high temperatures. The region of the validity is indicated by the solid line. Its continuation (black dashes) shows the asymptotic behavior of our model at high temperatures. The results of PIMC method and FVT are also shown.

is an approximation for the determination of the direct correlation function, the results for the EOS calculated within the HNC+MAL method agree very well with those from the REMC method. We see that the HNC+MAL can be used to describe shock compressed systems in a wide range of temperatures and densities.

In order to improve the partition function for molecular hydrogen (deuterium) we have calculated rotational and vibrational energy levels by solving the Schrödinger equation with the potential Eq. (5) calculated by Kolos and Wolniewicz [39]. The resulting partition function was used in the expression for the dissociation constant and for the internal energy. Comparing results for the degree of dissociation α , calculated by using the expression for dissociation constant Eq. (6) and the one within the harmonic oscillator approximation, we have found that the latter overestimates the formation of molecules at high temperatures. It leads to shifting the Hugoniot curve to higher densities with wrong asymptotic behavior.

ACKNOWLEDGMENTS

The authors wish to thank H. Juranek and R. Redmer for helpful discussions and for providing the numerical data for the EOS and Hugoniot curve. We are grateful to V. Filinov for the discussion of details of Monte Carlo calculations. This work was supported by the Deutsche Forschungsgemeinschaft within the Sonderforschungsbereich 198: Kinetik partiell ionisierter Plasmen.

- [1] M. Schlanges and D. Kremp, *Ann. Phys. (Leipzig)* **39**, 69 (1982).
- [2] M. Ross, F.H. Ree, and D.A. Young, *J. Chem. Phys.* **79**, 1487 (1983).
- [3] D. Kremp, W.D. Kraeft, and A.J.D. Lambert, *Physica A* **127**, 72 (1984).
- [4] W. Ebeling and W. Richert, *Ann. Phys. (Leipzig)* **39**, 362 (1982); *Contrib. Plasma Phys.* **25**, 431 (1985).
- [5] P. Haronska, D. Kremp, and M. Schlanges, *Wiss. Zeitschr. Uni. Rostock, Math. Nat. Reihe* **36**, 98 (1987); M. Schlanges, M. Bonitz, and Tschtschtjan, *Contrib. Plasma Phys.* **35**, 109 (1995).
- [6] D. Saumon and G. Chabrier, *Phys. Rev. A* **44**, 5122 (1991); D. Saumon and G. Chabrier, *ibid.* **46**, 2084 (1992); D. Saumon, G. Chabrier, and H.M. Van Horn, *Astrophys. J.* **99**, 713 (1995).
- [7] G. I. Kerley, in *Molecular-Based Study of Fluid*, edited by J. M. Haile and G. A. Mansoori (American Chemical Society, Washington, 1983), pp. 107–138.
- [8] A. Bunker, S. Nagel, R. Redmer, and G. Röpke, *Phys. Rev. B* **56**, 3094 (1997); D. Beule, W. Ebeling, A. Förster, H. Juranek, S. Nagel, R. Redmer, and G. Röpke, *ibid.* **59**, 14177 (1999).
- [9] F.J. Rogers and D.A. Young, *Phys. Rev. E* **56**, 5876 (1997).
- [10] M. Ross, *Phys. Rev. B* **58**, 669 (1998); P. Arnault, J.M. Caillol, D. Gilles, P. Legend, F. Perrot, and F. Renard, *J. Phys. IV* **10**, 287 (2000).
- [11] H. Juranek and R. Redmer, *J. Chem. Phys.* **112**, 3780 (2000); H. Juranek, R. Redmer, and Y. Rosenfeld, *ibid.* **117**, 1768 (2002).
- [12] W.R. Magro, D.M. Ceperley, C. Pierleoni, and B. Bernu, *Phys. Rev. Lett.* **76**, 1240 (1996).
- [13] T.J. Lenosky, J.D. Kress, L.A. Collins, and I. Kwon, *Phys. Rev. B* **55**, R11907 (1997); T.J. Lenosky, J.D. Kress, and L.A. Collins, *ibid.* **56**, 5164 (1997).
- [14] G. Galli, R.Q. Hood, A.U. Hazi, and F. Gygi, *Phys. Rev. B* **61**, 909 (2000).
- [15] V.S. Filinov, M. Bonitz, and V.E. Fortov, *Pisma Zh. Eksp. Teor. Fiz.* **72**, 361 (2000) [*JETP Lett.* **72**, 245 (2000)].
- [16] S. Bagnier, P. Blottiau, and J. Clérouin, *Phys. Rev. E* **63**, 015301 (2000).
- [17] B. Militzer and D.M. Ceperley, *Phys. Rev. Lett.* **85**, 1890 (2000); B. Militzer, D.M. Ceperley, J.D. Kress, J.D. Johnson, L.A. Collins, and S. Mazevet, *ibid.* **87**, 275502 (2001).
- [18] B. Militzer and D.M. Ceperley, *Phys. Rev. E* **63**, 066404 (2001).
- [19] L.A. Collins, S.R. Bickham, J.D. Kress, S. Mazevet, T.J. Lenosky, N.J. Troullier, and W. Windl, *Phys. Rev. B* **63**, 184110 (2001).
- [20] M. Knaup, P.G. Reinhard, and C. Toepffer, *Contrib. Plasma Phys.* **41**, 159 (2001).
- [21] F. Gygi and G. Galli, *Phys. Rev. B* **65**, 220102 (2002).
- [22] L.B. Da Silva, P. Celliers, G.W. Collins, K.S. Budil, N.C. Holmes, T.W. Barbee, B.A. Hammel, J. D. Kilkenny, R.J. Wallace, M. Ross, R. Cauble, A. Ng, and G. Chiu, *Phys. Rev. Lett.* **78**, 483 (1997).
- [23] G.W. Collins, L.B. Da Silva, P. Celliers, D.M. Gold, M.E. Foord, R.J. Wallace, A. Ng, S.V. Weber, K.S. Budil, and R. Cauble, *Science* **281**, 1178 (1998).
- [24] W.J. Nellis, A.C. Mitchell, M. van Thiel, G.J. Devine, and R.J. Trainor, *J. Chem. Phys.* **79**, 1480 (1983).
- [25] N.C. Holmes, M. Ross, and W.J. Nellis, *Phys. Rev. B* **52**, 15835 (1995).
- [26] A.N. Mostovych, Y. Chan, T. Lehecha, A. Schmitt, and J.D. Sethian, *Phys. Rev. Lett.* **85**, 3870 (2000).
- [27] M.D. Knudson, D.L. Hanson, J.E. Bailey, C.A. Hall, J.R. Asay, and W.W. Anderson, *Phys. Rev. Lett.* **87**, 225501 (2001); M.D. Knudson, D.L. Hanson, J.E. Bailey, C.A. Hall, and J.R. Asay, *ibid.* **90**, 035505 (2003).
- [28] M. Ross and Lin H. Yang, *Phys. Rev. B* **64**, 174102 (2001).
- [29] W.R. Smith and B. Triska, *J. Chem. Phys.* **100**, 3019 (1994).
- [30] J.K. Johnson, A. Panagiotopoulos, and K.E. Gubbins, *Mol. Phys.* **81**, 717 (1994).
- [31] M. Lísal, W. Smith, and I. Nezbeda, *J. Chem. Phys.* **113**, 4885 (2000); M. Lísal, W.R. Smith, M. Bures, V. Vacek, and J. Navrátil, *Mol. Phys.* **100**, 2487 (2002).
- [32] J.K. Brennan and B.M. Rice, *Phys. Rev. E* **66**, 021105 (2002).
- [33] H.E. DeWitt and F.J. Rogers, *Phys. Lett. A* **132**, 273 (1988); K. Ng, *J. Chem. Phys.* **61**, 2680 (1974).
- [34] D. Levesque, J. Weiss, and G. Chabrier, *J. Chem. Phys.* **94**, 3096 (1991).
- [35] J. O. Hirschfelder, C. F. Curtiss, and R. B. Bird, *Molecular Theory of Gases and Liquids* (Wiley, New York, 1967).
- [36] F. H. Ree, in *Shock Waves in Condensed Matter*, edited by S. C. Schmidt and N. C. Holmes (Elsevier, New York, 1988) p. 125.
- [37] T. L. Hill, *Statistical Mechanics* (McGraw-Hill, New York, 1956).
- [38] P. M. Atkins and R. S. Friedman, *Molecular Quantum Mechanics* (Oxford University Press, Oxford, 1997).
- [39] W. Kolos and L. Wolniewicz, *J. Chem. Phys.* **43**, 2429 (1965).
- [40] X.L. Liu, L. Su, and P. Ding, *Int. J. Quantum Chem.* **87**, 1 (2002).
- [41] G. Herzberg and L.L. Howe, *Can. J. Phys.* **37**, 636 (1959).
- [42] B.P. Stoicheff, *Can. J. Phys.* **35**, 730 (1957).
- [43] R.W. Patch, *J. Quant. Spectrosc. Radiat. Transf.* **9**, 63 (1968).
- [44] L. Wolniewicz, *J. Chem. Phys.* **45**, 515 (1966).
- [45] T.G. Waech and R.B. Bernstein, *J. Chem. Phys.* **46**, 4905 (1967).
- [46] W. Ebeling, W. D. Kraeft, and D. Kremp, *Theory of Bound States and Ionization Equilibrium in Plasmas and Solids* (Akademie-Verlag, Berlin, 1976).
- [47] K. P. Huber and G. Herzberg, in *NIST Chemistry Webbook, NIST Standard Reference Database Number 69*, edited by P. J. Linstrom and W. G. Mallard (National Institute of Standards and Technology, Gaithersburg, MD, 2001) (<http://webbook.nist.gov>).
- [48] M. P. Allen and D. J. Tildesley, *Computer Simulations of Liquids* (Clarendon, Oxford, 1987).
- [49] J.P. Hansen, G.M. Torrie, and P. Vieillefosse, *Phys. Rev. A* **16**, 2153 (1977); L.L. Lee, *J. Chem. Phys.* **97**, 8606 (1992).
- [50] M.J. Gillan, *Mol. Phys.* **38**, 1781 (1979).
- [51] W.J. Nellis, A.A. Louis, and N.W. Ashcroft, *Philos. Trans. R. Soc. London, Ser. A* **356**, 119 (1998).
- [52] S.T. Weir, A.C. Mitchell, and W.J. Nellis, *Phys. Rev. Lett.* **76**, 1860 (1996).
- [53] J.D. Johnson, *Phys. Rev. E* **59**, 3727 (1999).
- [54] D. Beule, W. Ebeling, A. Förster, H. Juranek, R. Redmer, and G. Röpke, *Phys. Rev. E* **63**, 060202 (2001).
- [55] W.J. Nellis, *Phys. Rev. Lett.* **89**, 165502 (2002).

- [56] J. E. Mayer and M. G. Mayer, *Statistical Physics* (Wiley-Interscience, New York, 1977).
- [57] H. Juranek, R. Redmer, and W. Stolzmann, *Contrib. Plasma Phys.* **41**, 131 (2001).
- [58] G.W. Collins, P.M. Celliers, L.B. Da Silva, R. Cauble, D.M. Gold, M.E. Foord, N.C. Holmes, B.A. Hammel, R.J. Wallace, and A. Ng, *Phys. Rev. Lett.* **87**, 165504 (2001).
- [59] S. I. Belov, G.V. Boriskov, A.I. Bykov, I. Il'kaev, N.B. Luky'anov, A.Ya. Matveev, O.L. Michailova, V.D. Selemir, G.V. Simakov, R.F. Trunin, I.P. Trusov, V.D. Urlin, V.E. Fortov, and A.N. Shuikin, *Pisma Zh. Eksp. Teor. Fiz.* **76**, 508 (2002) [*JETP Lett.* **76**, 433 (2002)].